DESIGN OF A TRI-AXIAL MICRO PIEZOELECTRIC ACCELEROMETER

Rui-hua HAN, Jian-yan WANG, Ma-hui XU, Hang GUO*

Pen-Tung Sah Institute of Micro-Nano Science and Technology of Xiamen University, Fujian, 361005, China
*Corresponding author, E-mail: hangguo@xmu.edu.cn.

A piezoelectric accelerometer based on bulk micromachining was presented in this paper. It is composed of a mass block and four cantilever beams with PZT piezoelectric thin films for detection deposited on cantilever beams. In order to realize the multi-axis detection with a single mass block, beam deformations due to the acceleration in X, Y, Z-axis directions were discussed to determine the corresponding connections of sensing elements. Analytical model was fundamentally derived and analyzed. Based on these, finite element method in ANSYS was used to design a tri-axial micro piezoelectric accelerometer. Parameters of the micro piezoelectric accelerometer, including the length, width and thickness of the cantilever beam and thickness of the PZT thin film, were optimized to acquire high charge sensitivity and wide bandwidth. Results showed that charge sensitivity along the X, Y, Z-axis could reach up to 23.85pC/g, 4.62 pC/g and 4.62pC/g, respectively, and the fundamental natural frequency up to 230.46Hz, for the presented micro piezoelectric accelerometer.

Keywords: Micro piezoelectric accelerometer; Triaxial detection; Natural frequency; Charge sensitivity

1. INTRODUCTION

Due to the rapid development in the micro electro mechanical system (MEMS) technology in past decades, various types of micro accelerometers have been proposed and developed. Micro accelerometers are generally classified into piezoresistive, capacitive, thermal, and resonant types [1]. Compared with other types of accelerometers, micro piezoelectric accelerometers have advantages of low power consumption, high sensitivity, less temperature dependence, and high bandwidth. These attractive properties of micro piezoelectric accelerometers posed great potential in many fields such as aerospace, automatic control, and biomedical engineering [2-5]. Many research groups paid great efforts in developing micro piezoelectric accelerometers. DeVoe et al used surface machining technology to develop a zinc oxide (ZnO) thin film piezoelectric accelerometer [6]. To enhance the sensitivity of the micro accelerometer, Saayujya et al used bulk micromachining technology to develop a ZnO thin film piezoelectric accelerometer [7]. In our previous work [8-10], the piezoelectric thin film single axis accelerometers by using bulk micromachining technology and growth of PZT thin film by using sol-gel method, had been studied.

In order to solve multi-axis detection with a single mass block, a tri-axis bulk-micromachined PZT thin film piezoelectric accelerometer was presented and designed in this work. The fundamental and structure of the micro piezoelectric accelerometer, especially the electrode connections for realizing tri-axis detection, were studied, and its geometrical parameters were optimized to acquire high charge sensitivity and wide bandwidth, with a target of being used in aerospace engineering.

2. PRINCIPLE AND STRUCTURE

The principle of micro piezoelectric accelerometer is shown in Fig.1. The piezoelectric thin film as the sensing element is located on the surface of the fixed end of the silicon cantilever beam, and a mass black is at the free end of the beam. When the accelerometer is subjected to an external loading, there would be a displacement in the mass block and the cantilever beam would produce a deformation. Thus, the piezoelectric thin film sensing element will experience tensile or compressive stress and generate an electric charge or voltage on its surface due to the piezoelectric effect, i.e. the piezoelectric coefficient d_{31} of the thin film.

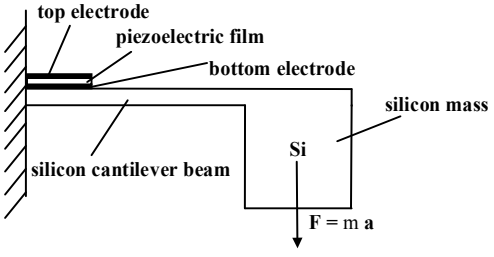

Figure 1. Principle schematic of the piezoelectric accelerometer

The structure and distribution of sensing elements for detecting the tri-axis acceleration of our micro piezoelectric accelerometer is shown in Fig.2. It can be fabricated on a SOI wafer by using the bulk micromachining technology. The square silicon mass

978-1-5090-1189-6/16/$31.00 ©2016 IEEE

block is suspended by four silicon cantilever beams that are symmetrically distributed in a cross shape. The PZT piezoelectric thin film with top and bottom electrodes are deposited on the silicon cantilever beams and each beam has two marked piezoelectric thin film sensing elements. Totally, there are eight sensing elements on the four silicon cantilever beams, where the sensing elements Z_1, Z_2, Z_3, and Z_4 are for detecting the acceleration in the Z-axis direction, X_1 and X_2 for X-axis direction, and Y_1 and Y_2 for Y-axis direction, respectively. Figure 3 shows the silicon beam deformation and connection of electrodes of sensing elements for detecting the acceleration along the Z-axis and X-axis direction, respectively. The sensing elements Z_1, Z_2, Z_3, and Z_4 are connected in parallel, leading to a charge or voltage signal V_z to be output between their top and bottom electrodes, while the signal V_x is output from top electrodes of the sensing elements X_1 and X_2, and the signal V_y from the top electrodes of the sensing elements Y_1 and Y_2 [9].

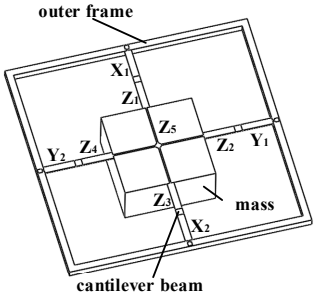

Figure 2. Schematic view of the micro piezoelectric accelerometer

It can be seen from Fig. 3(a) that the four silicon beams experience the same bending deformation when the Z-axis acceleration is applied. The compression deformation occurs at Z_1, Z_2, Z_3, Z_4. As a consequence, they produce the charge with the same polarity. Since they are in parallel connection, the potential difference V_Z is not zero. Meanwhile, tensile deformation occurs at X_1, X_2, Y_1, Y_2, resulting in tensile stress and charge with the same polarity. Because they are symmetrically distributed, the amount of charge generated is equal. So the potential difference V_x between X_1, X_2 is zero, and the potential difference V_y between Y_1, Y_2 is zero too. This means that the detection of Z-direction acceleration avoids the X-direction and Y-direction interference. As shown in Fig. 3(b), when the X-direction acceleration is applied, tensile deformation occurs at X_1 but compression deformation at X_2. Therefore, X_1 and X_2 produce the charge with the opposite polarity. Also, at this time, there is a compression deformation at Z_2 and a tensile deformation at Z_4, resulting in their opposite polarity of charge. Meanwhile, there is torsion deformation in the Y-direction, shear stress may occur but they are so weak that the generated charges can be neglected. Therefore, only the potential difference V_x is not zero, but V_y, V_z are zero. Thus, jamming in Y- direction and Z-direction can be avoided when detecting the acceleration in *x*-direction. The principle of acceleration in *Y*-direction is the same as that of *X*-direction.

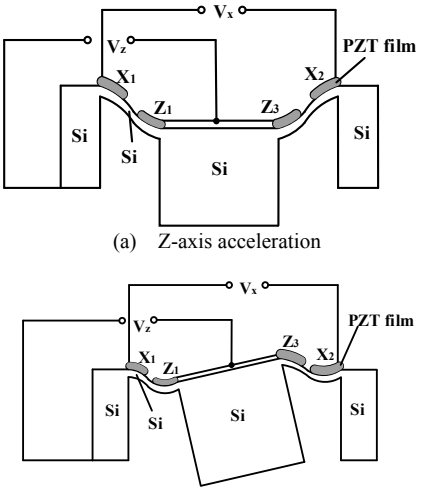

Figure 3. Schematic diagram of cantilever beam deformation and sensing elements connection for the micro piezoelectric accelerometer

3. THEORETICAL ANALYSIS AND DESIGN

Sensitivity and bandwidth are two important parameters in evaluating the performance of the accelerometer. In our study, the PZT thin film is used as sensing since it has higher piezoelectric coefficient than ZnO and other piezoelectric materials. It can produce a large amount of charges under the same deformation that is beneficial to improve the sensitivity of the micro piezoelectric accelerometer.

In order to fundamentally set up the analytical model of the micro piezoelectric accelerometer, several assumptions are put forward as follows: (1) The mass of cantilever could be ignored, compared with that of the central seismic mass; (2) The thickness of the top and bottom electrodes of the PZT thin film can be ignored compared with that of the cantilever beam and PZT.

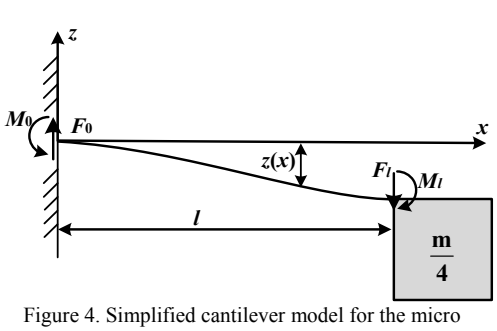

Figure 4. Simplified cantilever model for the micro piezoelectric accelerometer

978-1-5090-1189-6/16/$31.00 ©2016 IEEE

When the vertical acceleration is applied along the Z-axis, the stresses along the X- and Y- axis are so small relative to stress of the Z-axis that they can be neglected. Thus, the model for the micro piezoelectric accelerometer can be simplified as a cantilever that is shown in Fig. 4 [11-12].

The simplified structure was subjected to external forces F due to the acceleration in the Z-axis direction,

$$F = \frac{1}{4} m a_z \tag{1}$$

where m is the mass, and a_z the acceleration along Z-axis. The bending moment of the cantilever $M(x)$ is

$$M(x) = \frac{1}{4} m a_z (\frac{1}{2} l - x) \tag{2}$$

where l is the length of the cantilever.

Owing to the force and moment balance condition for the cantilever, we have

$$\int_{-(h-a)}^{a} bE_s \frac{z}{\rho} dz + \int_{a}^{h_{PZT}+a} bE_p \frac{z}{\rho} dz = 0 \tag{3}$$

$$\int_{-(h-a)}^{a} bE_s \frac{z}{\rho} z dz + \int_{a}^{h_{PZT}+a} bE_p \frac{z}{\rho} z dz = M(x) \tag{4}$$

where $E_S = E/(1-\nu^2)$, E and ν are the Young's modulus and the Poisson's Ratio of silicon, E_p the equivalent Young's Modulus of the PZT thin film along the longitudinal direction of the cantilever beam, a the distance from the interface of the PZT thin film and substrate to the neutral axis of the beam, b the width of the cantilever; h the thickness of the silicon beam, h_{PZT} the thickness of the PZT film, and ρ is the equivalent curvature radius of the cantilever beam and it can be derived from the above two equations.

The stress on the silicon beam at arbitrary position is

$$\delta_1 = \frac{E_p}{\rho} z = \frac{E_p M(x)}{EI_x} z \tag{5}$$

where Ix is the moment of inertia of the neutral plane relative to the X-axis. Since other stress is ignored, the electric displacement of PZT films at $z = h_{PZT} + a$ is achieved

$$D = d_{31}\delta_1 = d_{31} \frac{E_p M(x)}{EI_x} (\frac{h_{PZT}}{2} + a) \tag{6}$$

where d_{31} is the piezoelectric constant of PZT thin film. Then the amount of charge generated in the PZT films during vibration is

$$Q = \int_{0.55l}^{l} Dbdx = 0.031 d_{31} b \frac{E_p}{EI_x} (a + \frac{h_{PZT}}{2}) m a_z l^2 \tag{7}$$

The charge sensitivity is obtained as

$$K_q = 4gQ / a_z = 1.2152 d_{31} b \frac{E_p}{EI_x} (a + \frac{h_{PZT}}{2}) m l^2 \tag{8}$$

The fundamental natural frequency can be derived as the following equation by using the Rayleigh–Ritz method, which is

$$f = \frac{1}{2\pi} \sqrt{\frac{48 EI_x}{ml^3}} \tag{9}$$

With the formula fundamentally derived above, we can analyze and design the micro piezoelectric accelerometer. The length, width and thickness of the cantilever beam are initially set as 1000μm, 100μm and 1μm, respectively, and the thickness of the PZT film as 1 μm, and Table 1 shows the material properties for silicon and PZT that are used for the design of the micro piezoelectric accelerometer.

Table 1. Mechanical properties of silicon and the PZT in the micro piezoelectric accelerometer

	Silicon	PZT
Young's modulus, E (N/m²)	1.9×10^{11}	
Poisson's ratio, v	0.18	
Density (kg/m3)	2330	7550
Piezoelectric coefficient, d_{31} ($\times 10^{-12}$ C/N)		30
Seismic mass, m (kg)	1.165e-6	
Ep($\times 10^{10}$N/m²)		7.936

The charge sensitivity was calculated according to the formula as shown in Fig. 5(a). It can be seen that when the length of the cantilever beam was in the range from 700μm to 1200μm, the charge sensitivity increased with the increase of the length of the cantilever beam. While the first order natural frequency decreased with the increase of the length of the cantilever beam. When the width of the cantilever beam was in the range from 100μm to 150μm, the charge sensitivity was almost constant with the increase of the width of the cantilever beam, and the first order natural frequency increased with increase of width of the cantilever beam.

When the thickness of cantilever beam was in the range from 1μm to 6μm, the charge sensitivity decreased with the increase of the thickness of cantilever beam, the natural frequency increased with the increase of the thickness of beam (in Fig. 5(c)). When the thickness of the piezoelectric thin film PZT was in the range from 1μm to 6μm, the charge sensitivity decreased with the increase of the thickness

of the piezoelectric thin film PZT, while the first order natural frequency increased with the increase of the thickness of the piezoelectric thin film PZT.

The sensitivity highly depends on the piezoelectric performance of the PZT thin film. As shown in Fig.5 (e), when the piezoelectric coefficient d_{31} was in the range from 10 to 60 pC/N, the charge sensitivity is proportional to the piezoelectric coefficient, and sensitivity can be raised to nearly 60 pC/g.

Analytical formula is for simplified 1D structure, but the real accelerometer is 3D structure. Therefore, finite element method in ANSYS is used further analyze and design the practical structure of the micro piezoelectric accelerometer. The static mechanical analysis of ANSYS was conducted to simulate the force and the amount of electric charge when applied the acceleration. The image of static mechanics simulation was shown in Fig. 6. As can be seen in this figure, certain amount of charges was generated on the PZT film when it deformed.

The optimized length, width and thickness of cantilever beam was set as 1700μm, 250μm and 3.2μm, respectively, and thickness of PZT film was 0.9μm. Results of FEM in ANSYS showed that *z*-direction charge sensitivity along the Z-axis, X-axis and Y-axis were 23.85 pC/g, 4.62 pC/g, 4.62 pC/g, respectively, and fundamental frequency is d out to be 230.46 Hz. As a contrast, the above structural parameters were used to for calculation based on the fundamentally derived formulas, i.e. Eq. (8) and Eq.(9), and the sensitivity along the Z-axis was calculated to be 22.12pC/g, the first order natural frequency was calculated to be 207.47Hz. Apparently, the numerical analysis and analytical analysis results are well matched, indicating a reasonable numerical simulation. Curve of micro piezoelectric accelerometer in the 0-400 Hz frequency was shown in Fig. 6(b), no obvious peak could be observed when the frequency was lower than 230 Hz, and a clear peak emerged near 230 Hz. Thus, the sensitivity almost kept unchanged in the working bandwidth of 0-230 Hz.

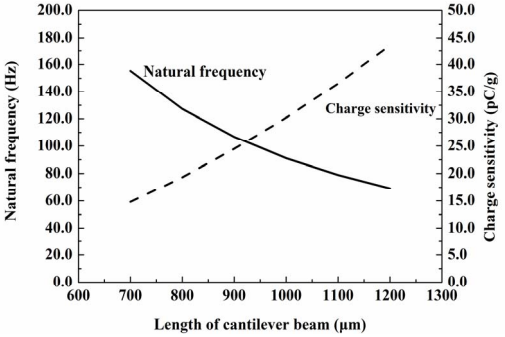

(a) With the change of the length of cantilever beam

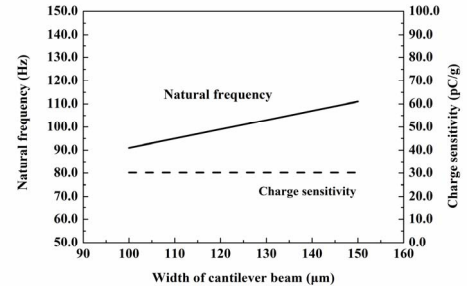

(b) With the change of the width of cantilever beam

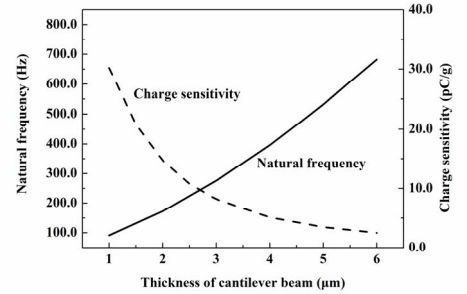

(c) With the change of the thickness of cantilever beam

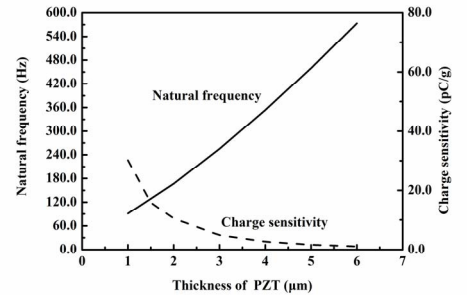

(d) With the change of the thickness of the piezoelectric film PZT

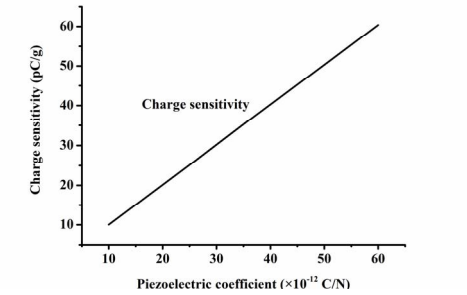

(e) With the change of the piezoelectric coefficient

Figure 5. Variation curve of the charge sensitivity and the first order natural frequency

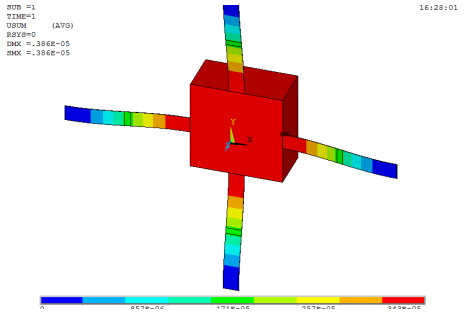

(a) The results of ANSYS simulation

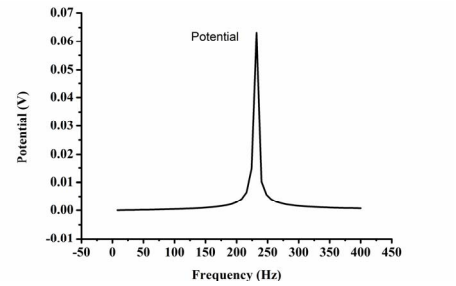

(b) Bandwidth curve of ANSYS analysis

Figure 6. Simulation in ANSYS

4. CONCLUSION

A tri-axis micro piezoelectric accelerometer was studied in this paper. Structure and working principle are explored in detail. Analytical model and finite element method in ANSYS are used to study the effects of geometric parameters and material properties on the performance of the micro piezoelectric accelerometer. In the end, the presented tri-axis micro piezoelectric accelerometer is designed to obtain the high sensitivity and wide bandwidth by optimizing its size parameters.

ACKNOWLEDGMENT

This work is financially supported by the Scientific Research and Development Program of City of Xiamen (3502Z20143003) and the Collaboration between Industry and University Program of Fujian Province (2015H6021).

REFERENCES

[1]. Narasimhan N, Li H, Miao JM. Micromachined high-g accelerometers: a review. *J. Micromech. Microeng.* 25(3): 033001, 2015.

[2]. Reus RD, Gulløv JO, Scheeper PR. Fabrication and characterization of a piezoelectric accelerometer. *J. Micromech. Microeng. 9*(9): 123-126, 1999.

[3]. Lynch JP, Partridge A, Law KH, et al. Design of piezoresistive MEMS-based accelerometer for integration with wireless sensing unit for structural monitoring. *Journal of Aerospace Engineering*. 16(3): 108-114, 2003.

[4]. Shen ZY, Tan CY, Yao K, Zhang L, Chen YF. A miniaturized wireless accelerometer with micromachined piezoelectric sensing elements. *Sensors and Actuators A: Physical*, 241:313-319,2016.

[5]. Cenk A, Andrei MS. Experimental evaluation of capacitive MEMS accelerometers. *J. Micromech. Microeng.* 13(5):634-635, 2003.

[6]. DeVoe DL, Pisano AP. A fully surface-micromachined piezoelectric accelerometer. *Technical Digest of Solid State Sensors and Actuators, 1997. TRANSDUCERS'97 Chicago., 1997 International Conference on. IEEE,* 2: 1205-1208, 1997.

[7]. Saayujya C. Design, fabrication and characterization of a Zinc Oxide thin-film piezoelectric accelerometer. *Proc. of IEEE 9th ISSNIP Symposium on sensor performance characterization,* 2014.

[8]. Yang H, Guo H. Design of A Bulk-Micromachined Piezoelectric Accelerometer. *Chinese Journal of Sensors and Actuators*, 21(2): 237-240, 2008.

[9]. Guo H, Bao DQ, Zhang Y. Characterization of PZT ferroelectric thin films prepared by a modified Sol-Gel method. *Proceedings of The 2008 IEEE Ultrasonics symposium*, 1-4:2130-2133, 2008.

[10]. Zhang Y, Feng P, Bao DQ, et al. Growth and characterization of lead zirconate titanate (PZT) thin films. *Optics and precision engineering,* 21(11): 2893-2899, 2013.

[11]. Wang QM, Yang ZC, Li F, et al. Analysis of thin film piezoelectric microaccelerometer using analytical and finite element modeling. *Sensors and Actuators A* 113:1–11, 2004.

[12]. Zou Q, Tan W, Kim ES, et al. Single- and Triaxis Piezoelectric-Bimorph Accelerometers. *J. Micromech. Microeng.* 17(1): 45-57, 2008.